Insights on radio frequency bilayer graphene FETs

G.Fiori, G. Iannaccone
Dipartimento di Ingegneria dell'Informazione
Università di Pisa, Via Caruso I-56122 Pisa, Italy
Tel. +39 050 2217639; Fax. +39 050 2217522, email: gfiori@mercurio.iet.unipi.it

***Abstract*— In this work, we investigate through atomistic simulations the possible improvements achievable by using bilayer graphene as FET channel material for radio frequency applications, and the related challenges. Bilayer graphene shows better performance as compared to monolayer graphene in terms of larger output resistance, which in turns is beneficial both for the low frequency voltage gain, and the maximum gain frequency.**

I. Introduction

Radiofrequency applications are considered with increasing interest for graphene-based transistors, as they seem to harness at best graphene's most promising properties (i.e., ultra high mobility and large saturation velocity), without suffering from its drawbacks (i.e. the absence of a band gap) [1], [2].

In analog electronics the FET is biased in inversion, therefore one can try to take full advantage of high mobility in order to have a high transconductance g_m and high cutoff frequency f_T. Recent experiments have shown $f_T \approx 155$ GHz for gate lengths of 40 nm [1] and a larger intrinsic (estimated) $f_T \approx 300$ GHz for nanowire gates [3].

However, the absence of band gap in graphene can have a negative impact also in analog applications: indeed, in short devices, where transport is quasi ballistic and drift velocity saturation cannot occur, interband tunneling suppresses the output differential resistance r_0 and therefore the intrinsic voltage gain $A_v = g_m r_0$. The lack of current saturation can be detrimental for the oscillator frequency f_{MAX}, i.e. the maximum frequency at which it is possible to obtain power gain. Recently, Szafranek *et al.* [4] have shown with experiments and simulation that a larger r_0 and A_v can be obtained by using bilayer graphene. The reason is that by applying an electric field perpendicular to the bilayer graphene plane it is possible to induce a gap of 100-200 meV. Even such a small gap, is sufficient to significantly improve saturation of the device output characteristics.

Here we provide through atomistic investigation, a physical insight of graphene bilayer FET for radio frequency application. To this aim we use our open source device simulator NanoTCAD ViDES [5], based on the self-consistent solution of the three-dimensional Poisson equation and of the Schrödingier equation with an atomistic tight binding Hamiltonian, within the non-equilibrium Green's functions formalism.

II. Results and discussion

We start from the structure considered in the experiments by Wu *et al.* [1], illustrated in Fig. 1. The bottom dielectric

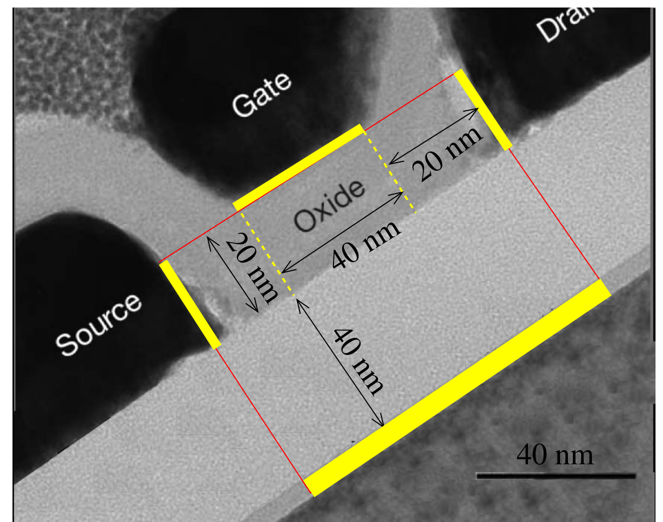

Fig. 1. Device structure of Ref. [1]: top oxide $t_{\mathrm{ox}} = 20$ nm, bottom oxide $t_{\mathrm{box}} = 40$ nm, spacer $t_{\mathrm{sp}} = 20$ nm.

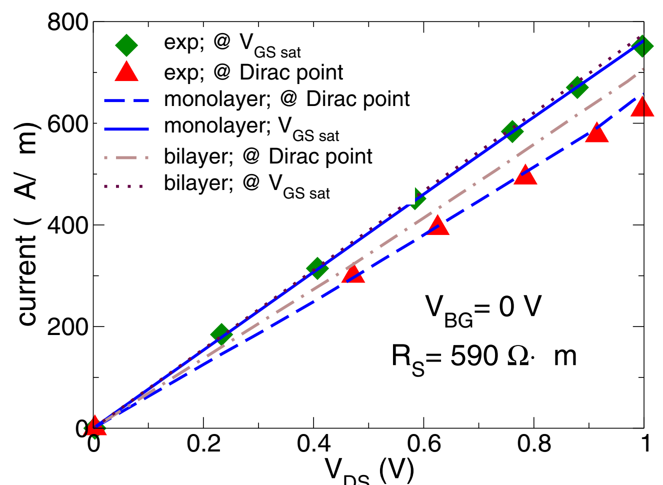

Fig. 2. Comparison of experimental and theoretical output characteristics considering $R_S = 590\ \Omega \cdot \mu$m for two different values of V_{GS}: source Fermi level at the Dirac point and $V_{GS} = V_{\mathrm{GSsat}}$ when current saturates as a function of V_{GS}.

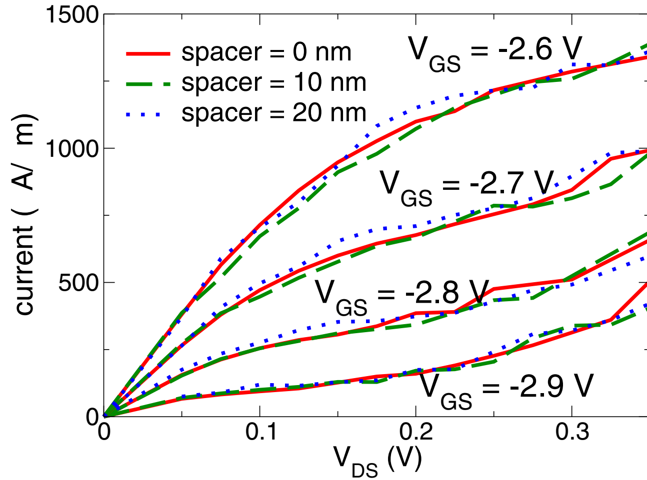

Fig. 3. Output characteristics of FET A with $t_{\text{ox}} = 4$ nm, $t_{\text{box}} = 40$ nm, lateral spacer $t_{\text{sp}} = 0, 10, 20$ nm, backgate voltage $V_{BG} = 40$ V, bilayer graphene channel. The spacer has no effect.

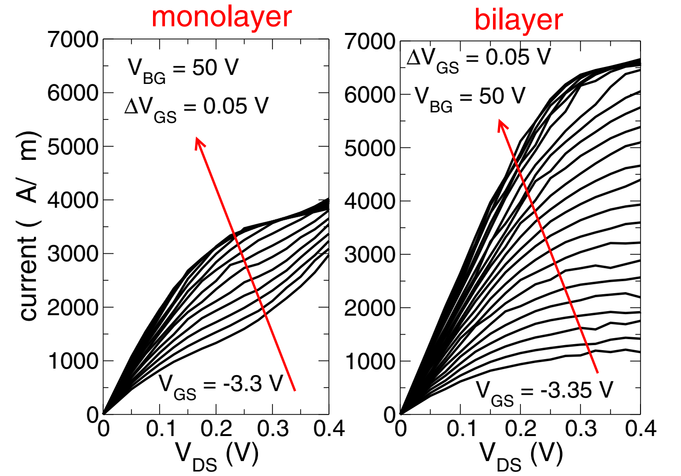

Fig. 4. Output characteristics of FET A with $V_{BG} = 50$ V with monolayer graphene channel (left) and bilayer graphene channel (right).

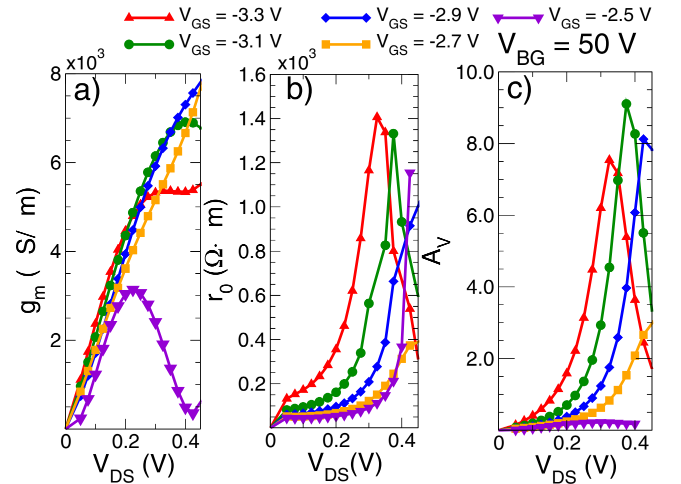

Fig. 5. Small signal transconductance g_m, output resistance r_0, and intrinsic gain A_v of FET A with $V_{BG} = 50$ V as a function of V_{DS} and V_{GS}. One should notice the degraded g_m for larger V_{GS} and the narrow peak in A_v as a function of V_{DS}.

layer consists of silicon oxide of thickness $t_{\text{ox}} = 20$ nm, the top dielectric layer is Al_2O_3 with thickness $t_{\text{box}} = 40$ nm.

Fig. 2 shows the measured output characteristics of the device shown in Fig. 1, when the channel is biased at the Dirac point and when current saturates as a function of V_{GS}. By comparing experiments with simulations performed with NanoTCAD ViDES we can extract the contact resistances at source and drain $R_S = 590\ \Omega \cdot \mu$m, which are in good agreement with experimental results [6]. As one can see in Fig. 2, the device exhibits very poor output characteristics for three main reasons:

- poor current saturation;
- large contact resistance;
- poor electrostatics due to large $t_{\text{ox}}/t_{\text{box}}$ ratio.

In order to understand the device potential performance and the improvements achievable with some band gap engineering, we can slightly modify the structure shown in Fig. 1 by substituting the monolayer graphene with bilayer graphene, and by applying a significant vertical electric field to the channel. In order to do so, we apply a large positive voltage V_{BG} on the backgate and, to improve electrostatics, we reduce the top oxide thickness t_{ox} to 4 nm. Let us call the resulting structure FET A.

The output characteristics of FET A, computed with $V_{BG} = 40$ V, for different values of the spacer layer t_{sp}, are shown in Fig.3. As can be seen, good saturation of the I_{DS}-V_{DS} characteristics is obtained. The spacer has no meaningful effect, given the large effective doping induced by V_{BG}.

To isolate and understand the improvements due to only bilayer graphene, we can consider the comparison in Fig. 4 between the output characteristics of two identical devices, biased with $V_{BG} = 50$ V, where the only difference is the use of monolayer graphene (left) or bilayer graphene (right) as channel. One can see the much improved current saturation and transconductance provided by bilayer graphene, even with a small bandgap (0.22 eV).

For the same device and same backgate voltage, small signal transconductance g_m, output resistance r_0, and intrinsic gain $A_v = g_m r_0$ are shown in Fig. 5 as a function of V_{DS} and V_{GS}. One can observe a promising maximum intrinsic gain, and two main drawbacks:

- as V_{GS} increases, we observe at some point a drastic fall in transconductance, due to a limited capacity of the contacts to inject mobile charge in the channel;
- A_v exhibits a narrow peak as a function of V_{DS}, which can cause distortion in the amplification or a reduced effective gain.

The backgate voltage is key to tune the energy band gap, and the main factor responsible for the high intrinsic gain achievable with bilayer graphene, as shown in Fig. 6. The larger the V_{BG}, the larger the bandgap, in turn the larger the intrinsic gain.

This concept is also clear from Fig.7 where a color map of the current density and the band edge profiles are shown for different bias points. If the band gap is too small, as in Fig.7a, interband tunneling is too large. If we increase the backgate voltage, the gap increases and interband tunneling

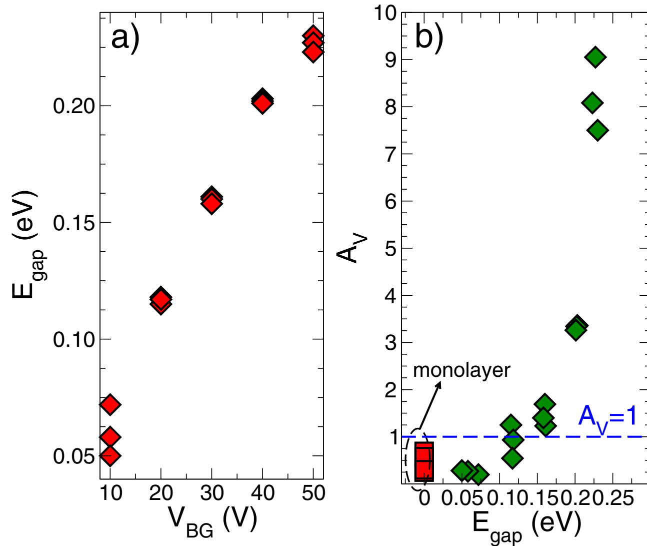

Fig. 6. Left: energy gap as a function of the backgate voltage for different V_{GS}; Right: intrinsic gain A_v as a function ofE_{gap} for different V_{GS}.

is suppressed, as shown in Fig.7b. With increasing V_{DS}, we reach a band edge profile that turns on interband tunneling again, reducing the output resistance (Fig.7c). Instead, if we increase V_{GS} we achieve current saturation, since current is limited by injection at the source (Fig.7d).

We also consider the achievable f_T and f_{MAX} of FET A (Fig. 8), including some non-idealities such as stray capacitances [7], and a varying contact resistance R_S from 0 to 590 $\Omega \cdot \mu$m. We assume zero gate resistance. For the bilayer graphene device discussed so far, for $R_S = 0$, we obtain f_T 1.5 THz and f_{MAX} $2 \div 4$ THz [8]. If a finite contact resistance is considered both f_T and f_{MAX} decrease, but for $R_S = 80\ \Omega \cdot \mu$m, as required by ITRS [9], we have both in the THz range.

Finally, in Fig. 9 we show the output waveform as a function of the input waveform for a very simple amplifier based on the FET whose characteristics are shown in Fig. 4. With a load of 500 $\Omega \cdot \mu$m the amplification is about -2 and distortion is negligible.

As a comparison with experimental results for different channel materials, in Fig. 10 we have added our data to Figure 1 of Ref. [10]. As can be seen, bilayer graphene devices with ideal contact resistances are promising with respect to traditional semiconductors for high frequency.

III. Conclusion

In this work, we have investigated through numerical simulations graphene bilayer Field Effect Transistors for analog applications. As compared to monolayer graphene FETs, bilayer graphene shows better current saturation due to the electrostatically induced band gap of up to 220 meV, sufficient to suppress interband tunneling and provide acceptable output resistance. This translates in a large voltage gain at low frequency and f_{max} in the THz regime, if contact resistances are reduced down to 80 $\Omega \cdot \mu$m.

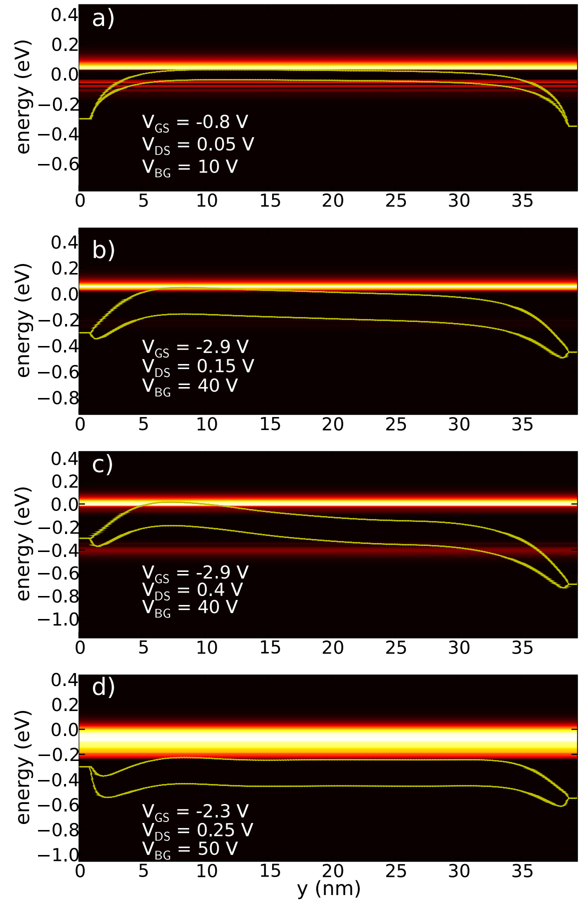

Fig. 7. Color plot of the current density of FET A for different bias points. In a) the gap is too small due to the low V_{BG} so that we observe interband tunneling, which is suppressed in b). In c) V_{DS} is so large the interband tunneling sets in. In d) current saturates as a function of V_{GS} due to limited injection from the source.

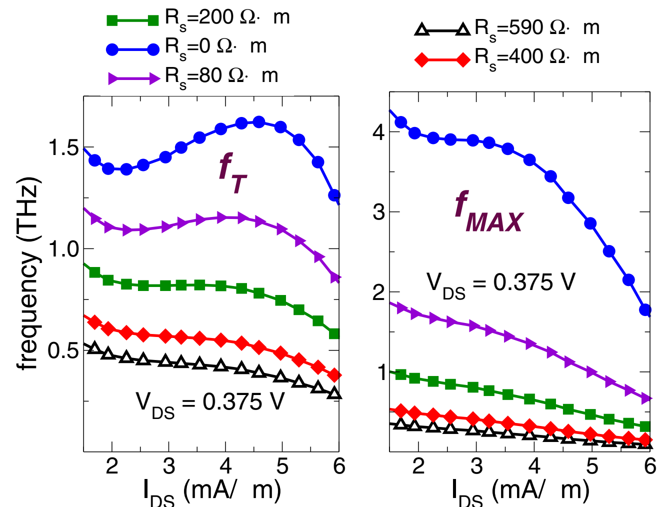

Fig. 8. f_T and f_{MAX} as a function of I_{DS} for FET A with $V_{BG} = 50$ V and different contact resistances.

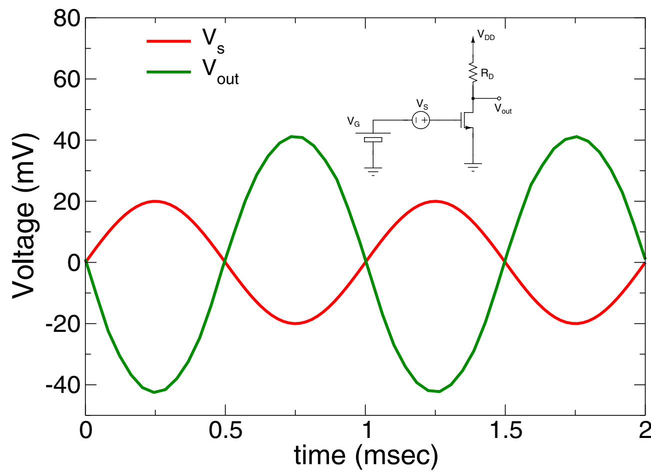

Fig. 9. Input and output waveform for the circuit in the inset considering the bilayer graphene FET and a load of 500 $\Omega \cdot \mu$m. No distortion is appreciable

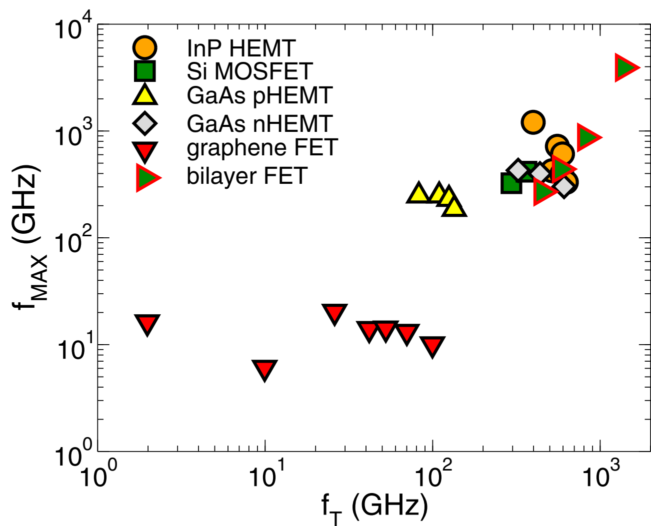

Fig. 10. Scatter plot of f_{MAX} and f_T considering data from Ref. [10] and Fig. 8.

IV. Acknowledgments

This work was supported in part by the EC Seventh Framework Program under the STREP project GRADE (Contract 317839) and by the MIUR-PRIN "Modeling and simulation of graphene nanoribbon FETs for high-performance and low-power logic applications" project (Prot. 2008S2CLJ9).

References

[1] Yanqing Wu, Yu-Ming Lin, Ageeth A Bol, Keith A Jenkins, Fengnian Xia, Damon B Farmer, Yu Zhu, and Phaedon Avouris, "High-frequency, scaled graphene transistors on diamond-like carbon", *Nature*, vol. 472, no. 7341, pp. 74–78, Apr 2104.

[2] G. Iannaccone, G. Fiori, M. Macucci, P. Michetti, M. Cheli, A. Betti, and P. Marconcini, "Perspectives of graphene nanoelectronics: Probing technological options with modeling", *Proc. of Int. Electr. Dev. Meeting*, pp. 245–248, 2009.

[3] L Liao, Y-C Lin, M Bao, R Cheng, J Bai, Y Liu, Y Qu, K L Wang, Y Huang, and X Duan, "High-speed graphene transistors with a self-aligned nanowire gate", *Nature*, vol. 467, pp. 305–308, 2010.

[4] B. N. Szafranek, G. Fiori, D. Schall, D. Neumaier, and H. Kurz, "Current saturation and voltage gain in bilayer graphene field effect transistors", *Nano Letters*, vol. 12, no. 3, pp. 1324–1328, 2012.

[5] "Available at http://www.nanohub.org/tools/vides. doi: 10254/nanohub-r5116.5".

[6] Y Wu and D Farmer, ", *Private Communications*.

[7] M I Elmasry, "Capacitance calulations of mosfet vlsi", *IEEE Electr. Dev. Lett.*, vol. 3, pp. 6–7, 1982.

[8] S M Sze and K K Ng, *Physics of Semiconductor Devices, Third Edition*, Wiley Interscience, third edition, 2006.

[9] "The international technology roadmap for semiconductors - 2011 edition - chapter 2: Process integration, devices, and structures. available at http://www.itrs.net".

[10] F. Schwierz, "Electronics: Industry-compatible graphene transistors", *Nature*, pp. 41–42, 2011.